Chinese Herbal Medicines 16 (2024) 121–131

Contents lists available at ScienceDirect

Chinese Herbal Medicines

journal homepage: www.elsevier.com/locate/chmed

Original Article

Effect of *Rhei Radix* et *Rhizoma* and *Eupolyphaga Steleophaga* on liver protection mechanism based on pharmacokinetics and metabonomics

Gang Feng [b,1], Jianli Bi [a,1], Wenfang Jin [a], Qi Wang [c], Zhaokui Dan [a,*], Baolei Fan [a,d,*]

[a] *Hubei University of Science and Technology, Xianning 437100, China*
[b] *The First People's Hospital of Xianning, Xianning 437000, China*
[c] *The First People's Hospital of Tongshan, Tongshan 437600, China*
[d] *Hubei Provincial Key Laboratory of Radiation Chemistry and Functional Materials, Xianning 437100, China*

ARTICLE INFO

Article history:
Received 26 May 2023
Revised 22 August 2023
Accepted 13 October 2023
Available online 18 December 2023

Keywords:
Dahuang Zhechong Pills
Eupolyphaga Steleophaga
^{1}H NMR
HPLC-MS/MS
metabonomics
pharmacokinetics
Rhei Radix et *Rhizoma*

ABSTRACT

Objective: Based on metabonomics technology of high-performance liquid chromatography-mass spectrometry (HPLC-MS/MS) and hydrogen nuclear magnetic resonance spectroscopy (^{1}H NMR), the pharmacokinetic characteristics and therapeutic mechanism of *Rhei Radix* et *Rhizoma* (RhRR, Dahuang in Chinese), *Eupolyphaga Steleophaga* (EuS, Tubiechong in Chinese) combined with RhRR acting on acute liver injury were explored.

Methods: Models of acute liver injury were established, and the pharmacokinetic methods of five components of RhRR-EuS in rats were found by HPLC-MS/MS. The liver tissues of different groups of mice were analyzed by ^{1}H NMR spectroscopy combined with multivariate statistical analysis to investigate the metabolomics of RhRR-EuS and RhRR.

Results: Pharmacokinetic results showed there were different levels of bimodal phenomenon in different groups, and the absorption of free anthraquinone in RhRR increased after compatibility with EuS. In addition, the pathological state of acute liver injury in rats can selectively promote the absorption of emodin, chrysophanol, physcion and aloe emodin. Through 15 differential metabolites in the liver tissue of acute liver injury mice, it was revealed that RhRR-EuS and RhRR could protect the liver injury by regulating the metabolism of glutamine and glutamic acid, alanine, aspartic acid and glutamic acid, and phosphoinositide. However, the regulation of RhRR was weaker than that of RhRR-EuS.

Conclusion: For the first time, we studied the pharmacokinetics and metabolomics differences of RhRR-EuS and RhRR in rats and mice with acute liver injury, in order to provide theoretical reference for clinical treatment of liver disease by DHZCP.

1. Introduction

Liver diseases refer to all diseases that occur in the organ of the liver, including autoimmune diseases, intrahepatic gallstones, neoplastic diseases, metabolic diseases, etc (Rezzani et al., 2019). It is well known that chronic liver disease is a global health problem (Cai et al., 2020). Therefore, the prevention and treatment of liver disease is of paramount importance. Traditional Chinese medicine (TCM) is unique in the treatment of liver diseases because of its long history and good therapeutic effect (Wu et al., 2022; Gao, Liu, An, & Ni, 2021; Li et al., 2022; Qian, Zhou, Shi, Pang, & Lu, 2023; Yang et al., 2021). Dahuang Zhechong Pills (DHZCP) is a famous prescription recorded in *Synopsis of the Golden Chamber* (Jingui Yaolue in Chinese) written by Zhongjing Zhang, a medical sage of Han Dynasty. It is widely used in the modern clinical treatment of hepatitis, cirrhosis and other patients with blood stasis (Wu et al., 2022; Zhang & Wang, 2019). As one of the classic ancient prescriptions, DHZCP is mainly composed of 12 herbs, including *Rhei Radix* et *Rhizoma* (Dahuang in Chinese), *Eupolyphaga Steleophaga* (Tubiechong in Chinese), *Hirudo* (Shuizhi in Chinese), *Tabanus* (Mengchong in Chinese), *Paeoniae Radix Alba* (Baishao in Chinese), *Persicae Semen* (Taoren in Chinese), *Scutellariae Radix* (Huangqin in Chinese), *Glycyrrhizae Radix et Rhizoma* (Gancao in Chinese) and etc, among which *Rhei Radix* et *Rhizoma* (RhRR) and *Eupolyphaga Steleophaga* (EuS) are recognized as the common monarch drugs (Wu et al., 2020). RhRR has the effect of activating blood circulation in compound DHZCP, while EuS is a blood-breaking drug, and both of them have the synergistic effect of invigorating

* Corresponding authors.
E-mail addresses: zkdan@163.com (Z. Dan), fanbl_1980@163.com (B. Fan).
[1] These authors contributed equally to this work.

https://doi.org/10.1016/j.chmed.2023.10.002
1674-6384/

blood and removing blood stasis. And the quality of these two herbs accounted for the highest proportion in the compound prescription.

In recent years, DHZCP has shown unexpected application effects in the adjuvant treatment of tumors (Ni et al., 2019; Tian et al., 2023). It is found that DHZCP has no obvious adverse reactions after long-term administration, and it is economical, effective and has broad application prospects (Chen et al., 2022; Gong et al., 2019). At present, the pharmacological effects of this ancient prescription are not clear, the main efficacy components are not clear, the application process lacks a unified standard and there are few relevant studies on the pharmacokinetics and metabolomics of DHZCP (Huang et al., 2021). Therefore, it is necessary to use modern technology and methods to further study the compatibility mechanism and main components of Chinese herbal medicines contained in DHZCP. In addition, the research of drug pair direction is widely used because of its small number of drug flavors, relatively simple research and the efficacy of reflecting the whole prescription. Pathology will make its pharmacokinetic parameters show significant differences to some extent (Tian et al., 2021). Therefore, the study of pharmacokinetic parameters and drug metabolism of drugs in pathological state is more relevant to clinic than that in normal state.

In this study, we selected RhRR and EuS as drug pairs. Under the pathological conditions of normal and acute liver injury, HPLC-MS/MS and ^{1}H NMR are used to conduct pharmacokinetic and metabolomics research, so as to further strengthen the research on the treatment of liver diseases with RhRR and EuS, and provide a more standardized and comprehensive scientific basis for the treatment of liver diseases.

2. Materials and methods

2.1. Materials

RhRR was purchased from Guangdong Lianfeng Traditional Chinese Medicine Pieces Co., Ltd. (Puning, China) and EuS was purchased from Bozhou Kangyiyin Biotechnology Co., Ltd. (Bozhou, China). RhRR and EuS were identified as the dried root and rhizome of *Rheum officinale* Baill. and the dried female body of *Eupolyphaga sinensis* Walker by associate professor Ruolei Xiao from School of Pharmacy, Hubei University of Science and Technology (No. 20230307).

2.2. Instruments

The following equipment was used in this experiment: Nuclear Magnetic Resonance instrument (AVANCE III, Bruker, Switzerland). Shimadzu LCMS-8040 high performance liquid chromatograph triple quadrupole mass spectrometer (HPLC-MS/MS) was purchased from Shimadzu Corporation (Jingdu, Japan). FA2004B electronic analytical balance was purchased from Shanghai Yueping Scientific Instrument Co., Ltd. (Shanghai, China). Electric digital display constant temperature water bath was purchased from Ningbo Yinzhou Qunan Experimental Instrument Co., Ltd. (Ningbo, China). RE-5299 rotary evaporator was purchased from Zhengzhou Yarong Instrument Co., Ltd. (Zhengzhou, China). SHZ-D(Ⅲ)circulating water multipurpose vacuum pump was purchased from Zhengzhou Boke Instrument Equipment Co., Ltd. (Zhengzhou, China). HR/T16M high-speed refrigerated centrifuge was purchased from Hunan Hexi Instruments Co., Ltd. (Changsha, China). KQ 3200DB numerical control ultrasonic cleaner was purchased from Kunshan Test Instrument Co., Ltd. (Kunshan, China). DZF-6050 vacuum drying oven was purchased from Shanghai Boxun Industrial Co., Ltd. (Shanghai, China). LGJ-10A freeze dryer was purchased from Shanghai Hefan Instrument Co., Ltd. (Shanghai, China). CM-RO-C2 laboratory ultra-pure water machine was purchased from Ningbo Sibodun Environmental Protection Technology Co., Ltd. (Ningbo, China).

2.3. Reagents

Rhein, emodin, chrysophanol, physcion, aloe emodin and 1,8-dihydroxyanthraquinone (IS) were purchased from Chengdu Efa Biotechnology Co., Ltd. (Chengdu, China), with more than 99% purity. The chemical structures and cracking mode of the main active components are shown in Fig. 1. Deuterium dimethyl sulfoxide (DMSO) was purchased from Shanghai McLean Biochemical Technology Co., Ltd. (Shanghai, China). Methanol and acetonitrile are chromatographic grade and purchased from Merk (Merck, Germany). The paraformaldehyde fixed solution (4%) and sodium heparin were purchased from Shanghai Macklin Biochemical Technology Co., Ltd. (Shanghai, China). Formic acid, glacial acetic acid, ammonia water and carbon tetrachloride are analytically pure. Formic acid was purchased from Tianjin Fuyu Fine Chemical Co., Ltd. (Tianjin, China). Glacial acetic acid and ammonia water were purchased from Tianjin Hengxing Chemical Reagent Manufacturing Co., Ltd. (Tianjin, China). Carbon tetrachloride was purchased from Tianjin Damao Chemical Reagent Factory (Tianjin, China). Olive oil was purchased from Shandong Dinghui Biotechnology Co., Ltd. (Weifang, China). Mobile phase water was Wahaha purified water.

2.4. Animals

A total of 24 male SD rats (8-week-old) weighing 200–220 g were included in the pharmacokinetic study. A total of 36 male KM mice (8-week-old) were included in the pharmacometabolomics study, with the body weight of 36–44 g. All the animals were placed in SPF animal room with temperature of (25 ± 0.5) °C and humidity of (50 ± 5)%. They were fed adaptively for 7 d with free drinking and eating, and the light circulated day and night for 12 h. All the animals were provided by Hubei Experimental Animal Research Center with the license number of SCXK (Hubei) 2015–0018. The animal program conforms to the Guide to Care and Practice of Laboratory Animals. The use of animals has been approved by the Animal Care and Use Committee of Hubei Institute of Science and Technology (Certificate No. SCXK (E) 2015–0018).

2.5. Preparation of solution

2.5.1. Preparation of reference standard solution

After 0.001 g of different reference substances were accurately weighed, a mixed reference substance stock solution with a concentration of 200 μg/mL was prepared with methanol and stored at 2–°C. 1,8-dihydroxyanthraquinone was selected as the internal standard (IS) of the active ingredient in RhRR-EuS drug pair, and the IS stock solution with the concentration of 200 μg/mL was prepared with methanol.

2.5.2. Preparation of sample decoction

The decoction was divided into RhRR and RhRR-EuS groups. In the RhRR group, 100 g of processed RhRR was weighed, immersed in seven times of water for 30 min, boiled, kept slightly boiling for 30 min, air-cooled and filtered. The residue was boiled again with six times of water, kept slightly boiling for 20 min, air-cooled and filtered. The decoctions were combined, and concentrated to 45 mL by rotary evaporation at 50 °C. According to the requirements of *Chinese Pharmacopoeia*, the clinical dose ratio of RhRR to EuS is 10:1 (Chinese Pharmacopoeia Commission, 2020). In the RhRR-EuS group, 100 g of processed RhRR and 10 g of processed EuS were

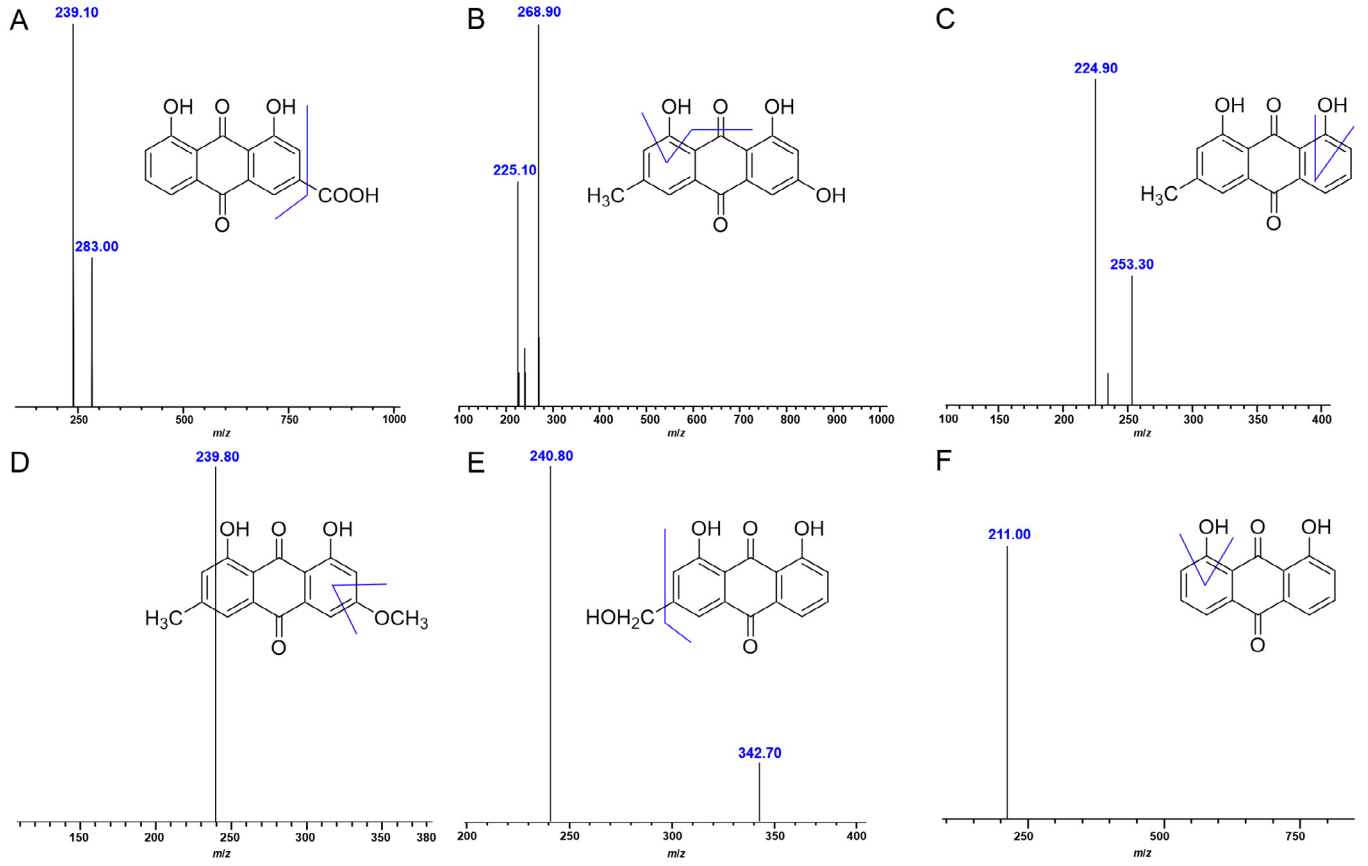

Fig. 1. Diagram of chemical structures and cracking mode of rhein (A), emodin (B), chrysophanol (C), physcion (D), aloe emodin (E) and 1,8-dihydroxyanthraquinone (IS) (F).

weighed, and the decocting process was the same as that in RhRR group.

2.6. Liquid chromatographic conditions

Sample were separated on an ODS-3 C_{18} column (250 nm × 4.6 mm, 5 μm), the mobile phase consisted of 0.1% aqueous ammonia solution (A) and pure methanol (B). Chromatographic separation was achieved with 85% B isocratic elution, the flow rate was 0.4 mL/min. Column temperature was maintained at 35 °C and sample injection volume was 5 μL.

2.7. Mass spectrometry conditions

Negative ion mode, MRM mode quantitative analysis, electrospray ionization (ESI) ion source, heating block temperature was 400 °C and DL temperature was 250 °C, electrospray voltage was 3.5 kV and atomizing gas flow rate was 3.0 L/min, drier flow rate was 15.0 L/min and collision gas pressure was 230 Kpa. The quantitative ion pairs of different components were shown in Table 1.

Table 1
Quantitative ion pair and collision voltage of compounds.

Compounds	Abbreviations	Quantitative ion pair	Collision voltage (V)
Rhein	Rh	283.1 > 239.1	−12
Emodin	Em	269.0 > 225.0	−27
Chrysophanol	Ch	253.1 > 225.0	−31
Physcion	Ph	283.1 > 240.1	−28
Aloe emodin	Ae	269.0 > 240.1	−20
1,8-Dihydroxyanthraquinone	IS	239.1 > 211.0	−20

2.8. Establishment of quantitative analysis method for each chemical component in plasma

2.8.1. Investigation on specificity of each chemical component in plasma and drawing of mass concentration standard curve

The specificity of the method was investigated by collecting blank plasma, blank plasma added with each chemical component, rat plasma sample in the RhRR group and rat plasma sample in the RhRR-EuS group, and operating according to the determination conditions under item 2.7.

A total of 50 mL of blank plasma, and the appropriate amount of each standard stock solution under item 2.5.1 was accurately measured. An appropriate amount of IS solution was added to prepare a series of plasma samples of each compound standard at 5, 10, 50, 100, 200, 500 and 1 000 ng/mL. The measurement conditions under item 2.7 were followed. With the concentration of each standdard (ng/mL) as x, the ratio of the corresponding component to IS as y, and the weighting coefficient of $1/x$, linear regression was performed to calculate the linear equation. The regression operation was performed using the weighted least squares method to draw the standard curve.

2.8.2. Investigation on precision, stability and recovery of each chemical component in plasma

A volume of 200 μL rat blank plasma was added with different mass concentrations of compound standard solution to pre-

pare low (10 ng/mL), medium (100 ng/mL) and high (500 ng/mL) samples, respectively. The intra-day and inter-day precision were investigated. The stability of each chemical component in plasma of the samples with three concentrations was investigated after they were stored at room temperature for 24 h, stored at 4 °C for 14 d, and frozen at − 20 °C for 15 d. The standard solutions with three mass concentrations were prepared by dissolution in methanol, and the peak areas of each compound in plasma and methanol were compared to investigate the matrix effect of three chemical components in rat plasma. The recovery rate of sample addition was calculated according to the following formula:

$$\text{Recovery rate}\ (\%) = \frac{\text{Actual measured drug concentration}}{\text{Actual drug concentration prepared}} \times 100$$

2.9. Pharmacokinetic studies on active components in DHZCP

A total of 24 male SD rats [weighing (200 ± 20) g] were divided into four groups: two control groups and two model groups. The acute liver injury model was established in the model group. The rats were intraperitoneally injected with 50% CCl_4 olive oil solution at the dose of 3 mL/kg, and the rats in the control group were injected with the same volume of olive oil solution. During the establishment of liver injury model, all rats fasted but could drink water freely. After 12 h, the rats in each group were given RhRR-EuS and Rh decoction by intragastriction. The determination of the administered dose was mainly based on the equivalent dose ratio converted proportionally from different body surface areas of human and animals. The clinical dose of rats should be 1.3 times that of humans. The control group was given a single dose of

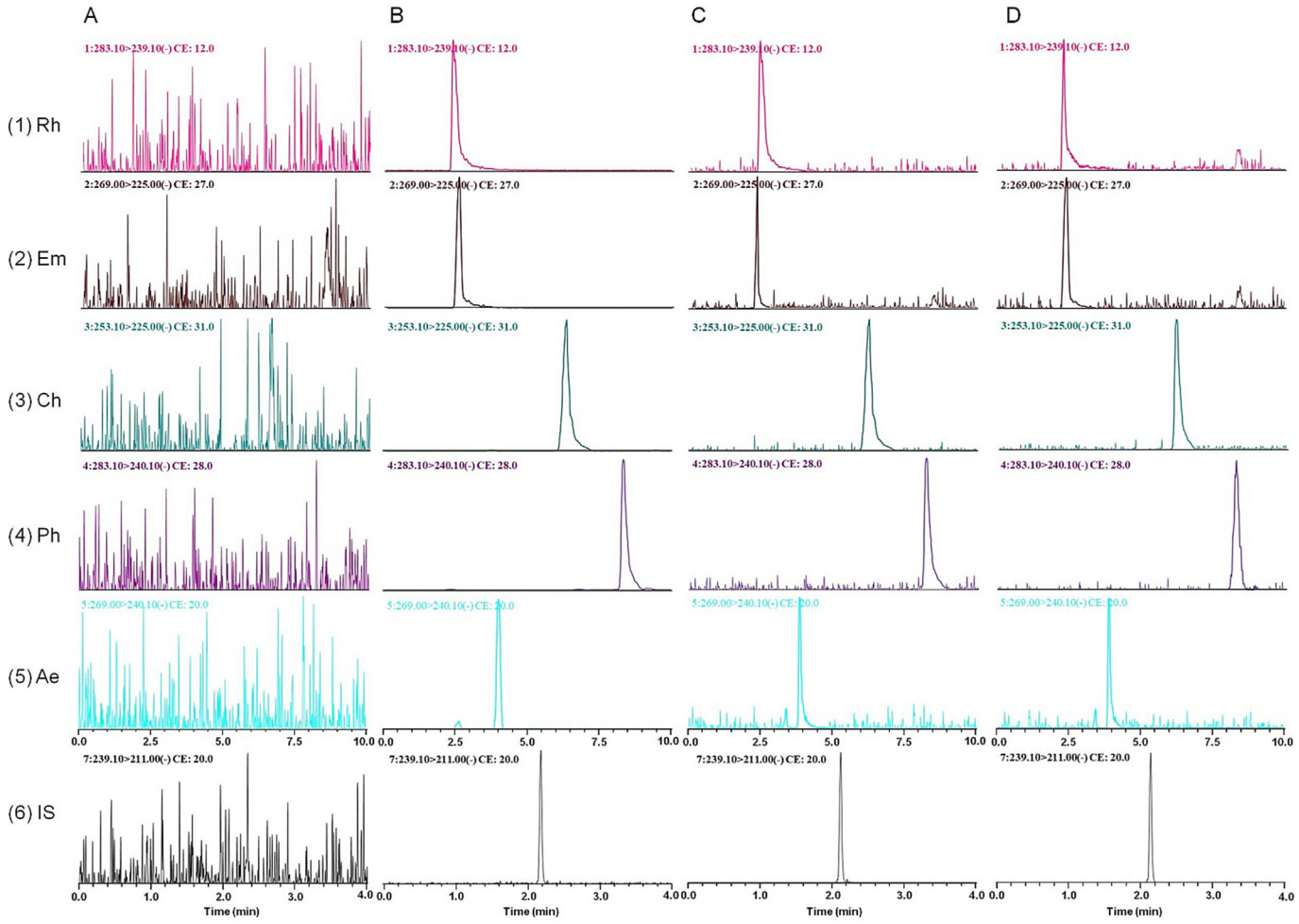

Fig. 2. Chromatogram of different compounds in rat plasma. A, blank plasma sample; B, blank plasma spiked with each reference substance and IS; C, plasma sample taken from rats in RhRR group; D, plasma sample taken from rats in RhRR-EuS group.

Table 2
Linear equation, Linearity range and LLOQ of different components in plasma.

Compounds	Linear equation	R^2	Linearity range (ng/mL)	LLOQ (ng/mL)
Rh	y = 0.056 6x + 0.326 7	0.995 7	5–1 000	5
Em	y = 0.060 8x + 0.330 9	0.997 0	5–1 000	5
Ch	y = 0.015 8x + 0.023 2	0.999 3	5–100 0	5
Ph	y = 0.016 8x + 0.004 0	0.995 6	5–1 000	5
Ae	y = 0.024 8x − 0.223 4	0.998 7	5–1 000	5

1.5 mL/200 g RhRR decoction and 1.5 mL/200 g RhRR-EuS decoction, while the model group was the same as the control group. Blood samples were collected from tail vein before (0) and 0.5, 1, 2, 4, 6, 8, 10 and 12 h after drug administration. A volume of 200 μL blood was placed in a centrifuge tube infiltrated with 1% sodium heparin and vortexed for 2 min. After centrifugation (12 000 r/min) for 10 min, 200 μL of the supernatant was blown dry under nitrogen flow. The residue was dissolved in 2 mL methanol, vortexed, and centrifuged to obtain the supernatant, which was filtered through a 0.22 μm organic membrane and stored at 4 °C for further analysis.

2.10. Metabonomics study on active components in DHZCP

A total of 36 male KM mice (weighing 20–22 g) were randomly divided into four groups, namely Control, Model, RhRR, and RhRR-EuS groups, with nine mice in each group. RhRR and RhRR-EuS groups were intragastrically administered with the corresponding dose of drug solution for one week, while Control group and Model group were given the same amount of normal saline. Two hours after the last administration, RhRR group, RhRR-EuS group and Model group were intraperitoneally injected with 10 mL/kg of 50% CCl_4 oil solution, while Control group was given the same amount of olive oil. After the experiment, all mice were fasted for 16 h, and three mice randomly selected were examined for pathological sections of liver tissue to determine the success of modeling. After successful inspection and modeling, all the mice were sacrificed after eyeball removal and bloodletting, and the liver tissues were taken out. After washed with normal saline, the liver was weighed, and added with an appropriate amount of cold normal saline (cold normal saline:liver = 9:1). The liver was cut into pieces, ground, homogenized, centrifuged (4 °C, 3500 r/min) for 15 min. The supernatant was lyophilized and stored at 4 °C for subsequent use.

The freeze-dried liver sample (5 mg) was added with 500 μL DMSO, vortexed to dissolution, centrifuged (4 °C, 10 000 r/min) for 10 min. A volume of 500 μL of the supernatant was transferred to 5 mm NMR tube for ^{1}H NMR analysis.

The liver tissue samples of each group were detected by NMR spectroscopy. The parameters acquired on the NMR spectrometer were as follows: frequency of 400 MHz, zg30 pulse sequence, scanning times of 16, spectral width of 8 012.8 Hz, pulse width of 10.26 Hz, sampling time of 4.089 4 s, relaxation delay of 3 s and temperature of room temperature.

2.11. Statistical analysis

The atrioventricular model was used to fit the plasma drug concentration data of rats after a single gavage administration, and PK Solver 2.0 software was used to calculate the pharmacokinetic parameters. All the data were statistically analyzed and plotted using Oringin and Microsoft Excel.

The nuclear magnetic resonance hydrogen spectrum was analyzed and processed by MestReNova professional software. Manual phase correction, baseline correction, and calibration with proton signals from lactic acid (δ = 1.33) were performed on the NMR hydrogen spectra, and metabolite identification for the ^{1}H NMR chemical shift was based on electronic databases HMDB (https://www.hmdb.ca/) and BMRB (https://www.bmrb.wisc.edu/). Taking δ 0.01 as a unit, performing segmental integration on the regions of δ 0.50–9.50 of all chromatograms. The effect of reagent peaks was removed. Finally, the total peak area integral data were normalized to the sum of 1, and the obtained data were converted into Excel tables, which were later used by Metabo Analyst (https://www.metaboanalyst.ca/) for statistical analysis.

Table 3
Investigation on precision, stability and sample recovery of each compound in plasma.

CC	C (ng/mL)	FC (ng/mL)	Precision investigation				Stability investigation								Matrix effect investigation		
			Intraday precision		Interday precision		Room temperature for 24 h			−4 °C for 14 d			−20 °C free for 15 d			FC (ng/mL)	R (%)	RSD (%)
			P (%)	RSD (%)	P (%)	RSD (%)	FC (ng/mL)	S (%)	RSD (%)	FC (ng/mL)	S (%)	RSD (%)	FC (ng/mL)	S (%)	RSD (%)			
Rh	10	10.01 ± 0.16	94.30	11.70	89.20	11.20	9.83 ± 0.05	106.20	9.13	9.90 ± 0.11	95.90	10.30	9.91 ± 0.11	109.40	5.83	10.98 ± 0.06	98.70	6.13
	100	98.08 ± 0.33	101.40	9.61	112.40	7.68	101.40 ± 0.13	112.30	4.32	100.80 ± 0.38	94.60	9.44	100.90 ± 0.41	95.30	8.62	99.64 ± 0.71	99.60	8.73
	500	501.31 ± 0.76	89.40	13.20	97.50	10.70	502.40 ± 0.53	89.40	10.50	501.90 ± 0.59	85.40	11.50	500.60 ± 0.46	100.40	9.64	501.55 ± 0.93	103.50	4.73
Em	10	10.05 ± 0.07	96.30	10.23	92.30	10.40	10.17 ± 0.47	104.60	5.95	10.06 ± 0.74	105	8.03	10.13 ± 0.84	98.50	7.65	9.86 ± 0.74	107	12.50
	100	101.27 ± 0.13	110.30	5.62	97.20	6.18	99.93 ± 0.53	110.40	5.84	99.54 ± 0.53	108	12.90	100.40 ± 0.738	108.40	8.58	100.80 ± 0.80	100.40	8.64
	500	502.01 ± 0.86	94.60	13.80	106.40	13.60	499.20 ± 0.74	99.60	13.40	500. 40 ± 0.50	89.90	6.87	499.60 ± 0.50	106	7.48	498.73 ± 0.96	98.50	2.76
Ch	10	10.17 ± 0.22	95.30	10.12	107.30	6.89	10.09 ± 0.07	114	6.78	10.11 ± 0.14	99.70	10.20	10.09 ± 0.11	105.40	9.08	10.38 ± 0.93	105.30	13.60
	100	102.02 ± 0.28	99.60	10.30	106.50	11.30	101.41 ± 0.71	105	9.74	100.95 ± 0.62	103	7.49	101.30 ± 0.78	102.30	9.36	101.17 ± 1.45	104.80	9.67
	500	500.01 ± 1.18	113	6.36	109.30	6.74	501.80 ± 0.84	90.40	6.62	500.90 ± 0.99	96.30	11.80	501.40 ± 0.98	99.50	12.80	497.98 ± 0.93	104.90	10.37
Ph	10	9.78 ± 0.48	112.90	4.93	94.70	10.40	9.97 ± 0.79	103	5.87	10.10 ± 0.63	99.50	9.70	10.40 ± 0.46	105	8.93	10.56 ± 0.12	106.90	9.67
	100	101.81 ± 0.82	99.80	13.50	100.60	13.50	98.94 ± 0.59	105	8.97	99.06 ± 0.75	102	7.94	100.10 ± 0.59	100.6	9.48	98.93 ± 0.56	99.60	4.78
	500	499.92 ± 0.79	93.50	11.70	104	12.50	500.50 ± 1.03	90.50	6.83	499.90 ± 0.89	96.70	11.40	499.40 ± 0.95	95.3	12.50	502.30 ± 1.29	100.64	3.24
Ae	10	10.10 ± 0.99	106.20	8.79	100.40	9.81	10.19 ± 0.08	99.60	11.90	10.05 ± 0.12	107	13.10	10.16 ± 0.83	88.6	6.83	10.48 ± 0.16	106.80	12.8
	100	98.87 ± 0.57	93.40	4.81	99.50	10.40	100.17 ± 0.69	88.50	9.53	100.80 ± 0.55	112	12.90	100.20 ± 0.63	84.3	9.34	100.37 ± 0.95	96.40	7.83
	500	501.39 ± 0.36	92.60	6.74	87.30	7.25	501.63 ± 0.88	98.50	9.26	500.76 ± 0.72	98.30	10.70	500.15 ± 0.95	85.6	12.5	500.74 ± 1.17	107.40	4.76

Note: CC, C, FC, P, S and R represent compound, concentration, found concentration, precision, stability and recovery respectively.

3. Results

3.1. Validation of a quantitative analysis method for compounds in plasma

3.1.1. Specifity

The sample diagram collected from blank plasma, blank plasma added with standard solution and plasma in rats after oral administration of RhRR and RhRR-EuS decoction was shown in Fig. 2. The retention times of rhein, emodin, chrysophanol, physcion, aloe-emodin and IS were 2.5, 2.5, 6.4, 8.3, 3.8, and 2.1 min, respectively. The five compounds and IS were detected with good peak shape and high resolution, and the endogenous components did not interfere with the analysis of the five components in the plasma sample.

3.1.2. Standard curve drawing of each compound in plasma

The standard curve was plotted based on X as the concentration (ng/mL) of each chemical component, the ratio of the corresponding component to the internal standdard (IS) as *y*, and the weighting coefficient of 1/*x*. Table 2. R^2 was within the range of 0.995 6–0.999 4, indicating good linearity over the range of 5–1000 ng/mL for each chemical component in plasma. The standard curve met the requirements for pharmacokinetic studies.

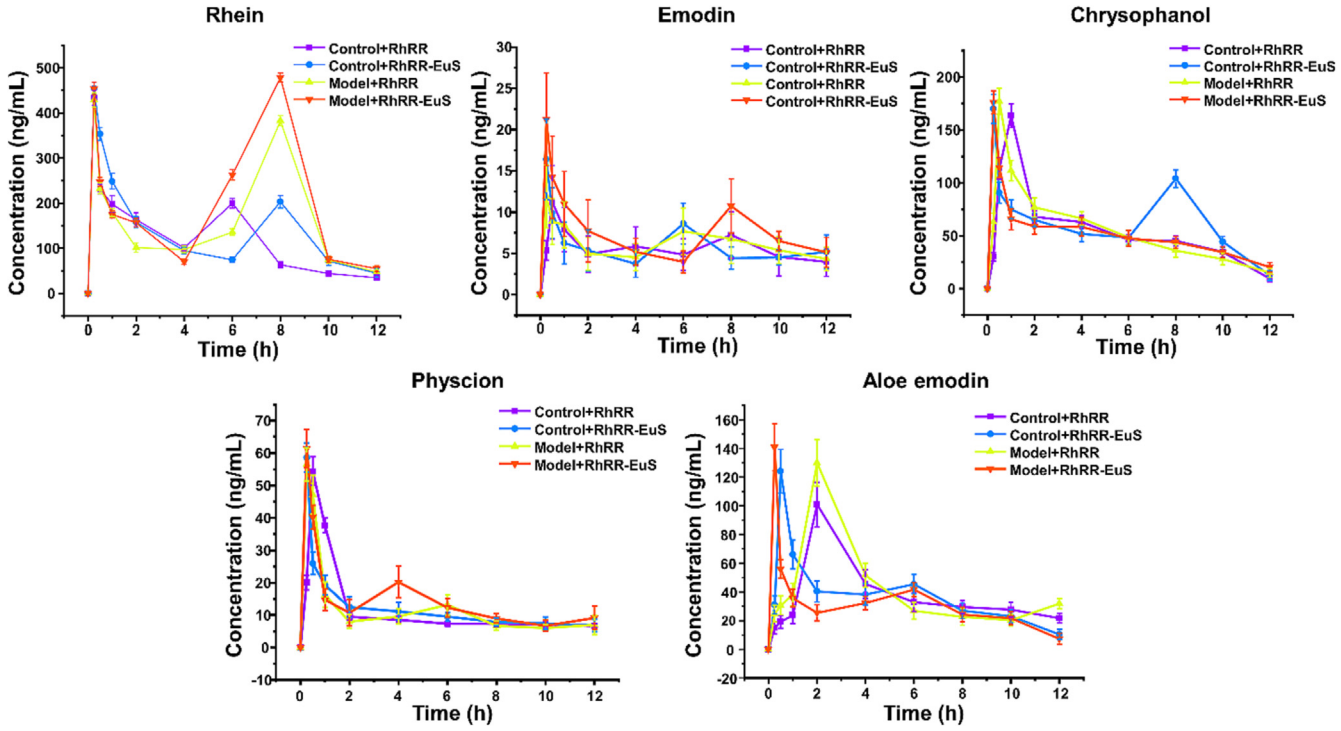

Fig. 3. Concentration-time profiles of different compounds after oral administration of RhRR and RhRR-EuS in rats.

Table 4
Pharmacokinetic parameters of different compounds in decoction of RhRR and RhRR-EuS in rats (n = 6).

Compounds	Groups	$AUC_{(0-t)}$ ((h·ng)/mL)	$AUC_{(0-i)}$ (h·ng/mL)	T_{max} (h)	C_{max} (ng/mL)	$T_{1/2}$ (h)	MRT_{0-t} (h)
Rh	RhRR of control group	1440.19	1671.79	0.25	433.78	4.61	6.31
	RhRR-EuS of control group	1604.41	1723.43	0.25	454.54	1.84	5.44
	RhRR of model group	1911.22	2003.74	0.25	428.60	1.34	6.19
	RhRR-EuS of model group	2401.27	2501.73	8.00	478.56	1.28	6.24
Em	RhRR of control group	67.68	94.10	0.50	11.18	4.62	9.30
	RhRR-EuS of control group	68.29	153.99	0.25	16.37	11.42	18.32
	RhRR of model group	73.14	112.30	0.25	11.9	6.26	11.07
	RhRR-EuS of model group	88.43	116.28	0.25	21.24	3.76	8.37
Ch	RhRR of control group	661.91	711.78	1.00	163.54	3.64	5.33
	RhRR-EuS of control group	739.17	762.71	0.25	169.98	1.31	5.64
	RhRR of model group	653.98	746.91	0.50	177.14	4.27	5.98
	RhRR-EuS of model group	612.76	717.61	0.25	176.11	3.59	6.59
Ph	RhRR of control group	135.70	414.29	0.50	54.42	28.75	37.33
	RhRR-EuS of control group	136.47	243.13	0.25	58.63	10.90	14.72
	RhRR of model group	134.23	182.73	0.25	56.53	4.80	8.29
	RhRR-EuS of model group	163.35	247.41	0.25	61.44	6.35	10.23
Ae	RhRR of control group	473.80	738.48	2.00	100.91	8.41	11.87
	RhRR-EuS of control group	442.80	488.81	0.50	124.11	3.04	5.78
	RhRR of model group	515.93	739.14	2.00	129.83	4.86	8.87
	RhRR-EuS of model group	368.67	396.36	0.25	140.84	2.61	5.63

3.1.3. Investigation on precision, stability and sample recovery of each compound in plasma

The results of precision, stability and recovery rate of each chemical component in plasma are shown in Table 3. Six samples were determined for each concentration. The precision, stability and recovery rate met the requirements of 80%–120%, with RSD < 20%. The results showed that the precision and stability of the method for the determination of each chemical component in plasma were good. The determination of drug concentration *in vivo* was not affected by the plasma matrix effect.

3.2. Pharmacokinetic study of acute liver injury before and after treatment

In this study, an HPLC-MS/MS method was established and successfully applied to the pharmacokinetic studies of five components in rats with normal and acute liver injury after oral administration of RhRR and RhRR-EuS decoctions. Through comparison, we found that the addition of EuS did affect the absorption of some components in RhRR. The mean plasma concentration–time curves (n = 6) of the five components after a single oral administration were shown in Fig. 3. The main pharmacokinetic parameters (AUC, T_{max}, C_{max}, $T_{1/2}$, and MRT) for the four groups were presented in Table 4. Fig. 3 showed that the pharmacokinetic characteristics of the five components are different between normal and acute liver injury rats after oral administration of RhRR and RhRR-EuS decoction, and there were double peaks in different degrees, so it is difficult to compare the parameters. Therefore, we chose the non-compartmental model to analyze the main parameters of each group truly and objectively (Hughes et al., 2019; Zheng et al., 2020), and the parameters were shown in Table 4. It was found that the bioavailability of rhein was the highest in all groups, and the AUC and C_{max} of most groups after oral RhRR-EuS were higher than those after oral Rh, indicating that the combination of RhRR-EuS could promote the absorption of five free anthraquinones, especially rhein.

3.3. Metabolomics study before and after treatment of acute liver injury

3.3.1. ^{1}H NMR analysis of live tissue

The metabolism of RhRR-EhS and RhRR in mice with liver injury was studied by ^{1}H NMR. There was no significant difference in the ^{1}H NMR spectra of liver tissue from each group, and a representative ^{1}H NMR spectrum was shown in Fig. 4. Based on the chemical shift, peak shape and coupling constant, combined with HMDB (https://www.hmdb.ca/) and BMRB (https://www.bmrb.wisc.edu/) databases (Li et al., 2020; Jing et al., 2022), liver metabolites were identified. A total of 46 metabolites were identified, including amino acids, organic acids, sugars, and choline metabolites (Table 5). The difference of liver metabolism in each group could not be determined only by the types of metabolites. The change of metabolite concentration needs to be further analyzed. As a highly quantitative technique, ^{1}H NMR can quantify and compare the identified metabolites by the integral area under each metabolite peak. The differences of metabolites before and after treatment for acute liver injury were comprehensively compared using multivariate statistical analysis.

3.3.2. Multivariate statistical analysis

PCA could be used to observe the overall distribution trend among all samples, reflecting the degree of variation between and within groups as a whole (Xiao et al., 2020; Yamamoto et al., 2021). The metabolite spectra of liver samples from each group were further characterized by PCA (Fig. 5A).

3.3.3. Screening of differential metabolites

PLS-DA metabolism analysis was performed among RhRR-EuS, RhRR, control and model groups to identify potential differential metabolites among each group (Fig. 5B–D). The samples in control group and model group were significantly separated, indicating that the liver injury model was successfully established in this study. The samples in RhRR-EuS group, RhRR group and model group were significantly separated. The model verification parameters R^2 and Q^2 in each group were greater than 0.9, which indicated that the model fitting effect was good and the reliability was high. The results show that the model has good fitting effect and high reliability. ^{1}H NMR data were analyzed by t-test, and liver metabolites with VIP > 1 and P < 0.05 were selected as differential metabolites (Wang et al., 2019; Li et al., 2018) (Table 6).

3.3.4. Analysis of metabolic pathways of acute liver injury and drug treatment in each group

The differential metabolites in liver tissue of each group shown in Table 6. Different metabolites were imported into the Metabo Analyst 5.0 database for pathway analysis (Li & Zhao, 2020). The metabolic pathways with P < 0.05 and Impact > 0.1 were selected as potential metabolic pathways (Fig. 5E–G).

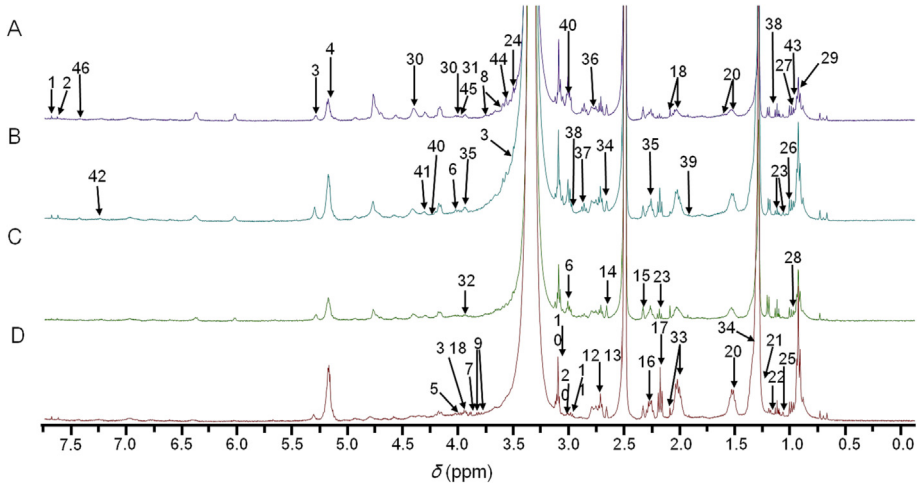

Fig. 4. ^{1}N NMR spectrum results of liver tissues in control group (A), model group (B), RhRR-EuS group (C) and RhRR group (D).

Table 5
Metabolite analysis of liver tissue in mice of different group.

No.	Metabolites	δ_H	Groups
1	UDP/UTP	7.97	RhRR, RhRR-EuS, K
2	Histidine	7.89(s)	RhRR, K
3	Glucose	5.45, 3.38(m), 3.96(dd)	RhRR, RhRR-EuS, K
4	Fatty acyl group	5.32	RhRR, M, K
5	Choline	4.08(s)	RhRR
6	Creatinine	4.04(s), 3.04(s)、	RhRR, RhRR-EuS, M, K
7	Serine	3.96(m)	RhRR, M, K
8	Aspartic acid	3.91(s), 2.81(dd)	RhRR, K
9	Betaine	3.89(s), 3.87(m)	RhRR
10	Cholamine	3.14(t)	RhRR, RhRR-EuS, M, K
11	α-Ketoglutaric acid	3.01(t)	RhRR
12	Dimethylamine	2.72(s)	RhRR, RhRR-EuS, M, K
13	Citrate	2.72(s)	RhRR, RhRR-EuS, M, K
14	Aspartate	2.67(dd)	RhRR, RhRR-EuS, K
15	Glutamine	2.34(m)	RhRR, RhRR-EuS, M, K
16	*p*-Cresol	2.26(s)	RhRR
17	Sodium butyrate	2.16(t)	RhRR
18	Proline	2.00(m), 2.07(m), 3.38(m)	RhRR, RhRR-EuS, M, K
19	Alanine	1.48(d)	RhRR, RhRR-EuS, K
20	Cadaverine	1.48(d), 1.49(d), 3.02(t)	RhRR, RhRR-EuS, M, K
21	3-Hydroxybutyric acid	1.23(d)	RhRR, RhRR-EuS, M, K
22	Isobutyrate	1.11(d)	RhRR
23	Valine	1.04(d), 0.99(d), 2.27(m)	RhRR、RhRR-EuS、M、K
24	Inositol	3.63(t)	K
25	α-Ketobutyrate	1.06(t)	RhRR
26	Deoxycholorine	0.93(s)	RhRR, RhRR-EuS, M, K
27	Isoleucine	0.93(t)	RhRR, RhRR-EuS, M, K
28	Isovaleric acid	0.91(d)	RhRR, M、K
29	Lipid	0.85(S)	RhRR, RhRR-EuS, M, K
30	Ascorbate	4.03(m), 4.53	RhRR-EuS, M, K
31	*N*-Acetylneuraminic acid	4.03(m)	RhRR-EuS
32	Hippuric acid	3.97	RhRR, RhRR-EuS, K, M
33	Glutamic acid	2.07(m), 2.17(m)	RhRR-EuS, M, K
34	Threonine	4.26(m), 1.22(d)	M, K
35	Acetone	2.25(s)	RhRR-EuS, K, M
36	DMA	2.76(m)	RhRR-EuS, K
37	Trimethyl amine	2.88(s)	RhRR-EuS, K
38	α-Ketoisovaleric acid	3.00(m), 1.07(d)	RhRR-EuS, K
39	Lysine	1.90(m)	RhRR-EuS, K
40	Lactic acid	4.11(q)	RhRR, RhRR-EuS, K, M
41	Adenosine	4.28(q)	RhRR-EuS
42	Tryptophan	7.21(t)	RhRR-EuS
43	LDL	0.89(m)	K
44	Glyceride	3.66(dd)	K
45	Glucose-6-phosphate	4.01(dd)	K
46	Phenylalanine	7.37(m)	K

Note: K, control group; M, model group; s, unimodal; d, double peak; t, triple peak; dd, double double peak; dt, double triple peak; m, multiple peaks.

3.4. Comparative analysis of pathological section of liver tissue in different groups

The liver tissue was fixed with 4% paraformaldehyde, embedded in paraffin, sectioned, and stained with hematoxylin and eosin (HE). The pathological results were shown in Fig. 6. The hepatic lobular structures of rats and mice in the control group were clear. Hepatic sinusoids and hepatic cords were normal, and there was no inflammatory cell infiltration. The pathological sections of liver tissues in the RhRR-EuS group, RhRR group and model group showed balloon-like lesions of hepatocytes to different degrees. The normal morphology of the nucleus disappears. Focal necrosis and inflammatory cell infiltration were observed locally. In summary, the liver injury in model group was successfully modeled compared with that in control group. The results in RhRR-EuS group and RhRR group indicated that RhRR-EuS and RhRR had different degrees of therapeutic effects on acute liver injury, while the therapeutic effect of RhRR-EuS was significant.

4. Discussion

In this study, a new pharmacokinetic method was established for the determination of five components in RhRR and EuS by HPLC-MS/MS. In particular, the effects of methanol–water, acetonitrile–water, methanol-0.1% formic acid water, methanol-5 mmol/L ammonium acetate and methanol-0.1% aqueous ammonia as the mobile phases on the resolution, peak shape and sensitivity of the measured chemical components were investigated. We found that methanol could improve the peak shape, and the signal of anthraquinone aglycone was relatively strong in the environment of 0.1% aqueous ammonia solution. Therefore, methanol-0.1% aqueous ammonia solution (E) was finally selected as the mobile phase.

The pharmacokinetic characteristics of the five components were analyzed after the first oral administration of the RhRR and RhRR-EuS decoctions to rats with normal and acute liver injury. Double peaks appeared in pharmacokinetics to different extents. Therefore, non-compartment model analysis was selected in this study to compare the main parameters among different groups. As shown in Fig. 4, enterohepatic circulation may be involved in the absorption process of these components. In addition, the double-peak phenomenon may also be caused by metabolic transformation between different tissues (Yu et al., 2017). The T_{max} of emodin, chrysophanol, physcion and aloe-emodin in model group was earlier than that in control group. It indicated that the effective components were more easily absorbed by the stomach and transfered into the blood after body injury. However, T_{max} of rhein in the control group was significantly delayed, indicating that the pathological state of acute liver injury in rats could selectively promote the absorption of certain components, and the specific absorption mechanism required further study. The AUC and C_{max} of most components after oral administration of RhRR-EuS were higher than those in the RhRR group, indicating that the absorption of free anthraquinone in the body was increased after the combination of Eu.

The liver metabolites of mice with acute liver injury before and after treatment were studied by ^{1}H NMR and characterized by PCA and PLS-DA methods. It was found that the content changes of 12 endogenous substances in the model group of mice were abnormal. It has been reported that CCl_4-induced liver injury is related to the formation and oxidation of free radicals (Wang et al., 2019; Zou et al., 2020), and the metabolism of amino acids is mainly carried out in the liver. Therefore, liver damage will inevitably cause amino acid metabolism disorder (An et al., 2019), and further lead to the increase of 3-hydroxybutyric acid, lactic acid, threonine, creatinine, valine, and trimethylamine in the Model group of mice. However, RhRR-EuS and RhRR can regulate them to normal levels through alanine, aspartic acid and glutamic acid metabolism, glycine, serine and threonine metabolism and other pathways. This indicated that RhRR-EuS and RhRR can reduce liver injury by regulating amino acid metabolism. Oxidative stress caused by CCl_4-induced liver injury can make collective energy supply disorder, anaerobic glycolysis activity significantly enhanced, and gluconeogenesis inhibition relieved, which leads to a significant decrease in glucose level and a significant increase in lactic acid level in the model group of mice (Miao et al., 2021). However, RhRR-EuS and RhRR could increase glucose levels and reduce lactic acid levels, indicating that they could enhance energy metabolism caused by liver injury. In addition, the synthesis of hippuric acid was performed by glycine and benzoic acid in the liver,

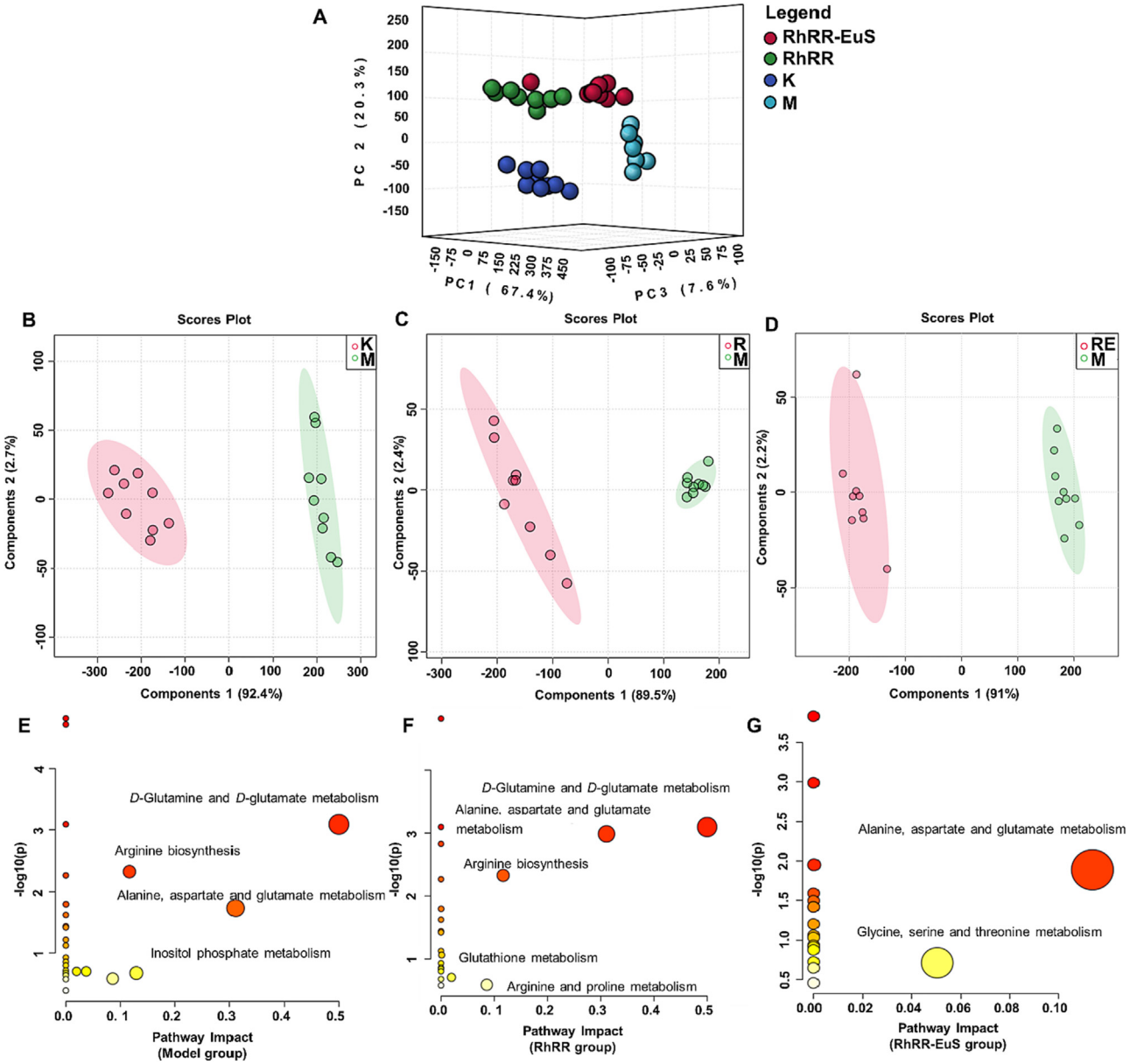

Fig. 5. Results of multivariate statistical analysis. A, PCA map of differential metabolites in different groups; B–D, comparison of metabolite in liver tissue of mice in each group; E–G, analysis of hepatic metabolic pathway in mice of each group (K, control group; R: RhRR group, RE: RhRR-EuS group; M, model group).

Table 6
Differential metabolites in liver tissue of mice in each group.

No.	Metabolites	*VIP*		
		K *vs* M	RhRR-EuS *vs* M	RhRR *vs* M
1	3- Hydroxybutyric acid	3.531↑	3.035↓	3.944↓
2	Glucose	3.295↓	3.018↑	2.677↑
3	Lactic acid	3.165↑	2.925↓	2.361↓
4	Threonine	2.889↑	–	–
5	Hippuric acid	2.790↓	2.908↑	2.225↑
6	Creatinine	2.340↑	2.277↓	2.094↓
7	Valine	2.164↑	2.054↓	1.868↓
8	Trimethyl amine	2.127↑	1.925↓	–
9	Isoleucine	2.081↓	1.908↑	1.772↑
10	Glutamine	1.079↓	1.304↑	1.689↑
11	Alanine	–	1.185↑	1.270↑
12	Glutamic acid	1.067↓	1.183↑	–
13	Adenosine	–	1.119↑	–
14	Betaine	–	–	1.156↑
15	Inositol	1.023↓	–	–

Note: K, control group; M, model group.

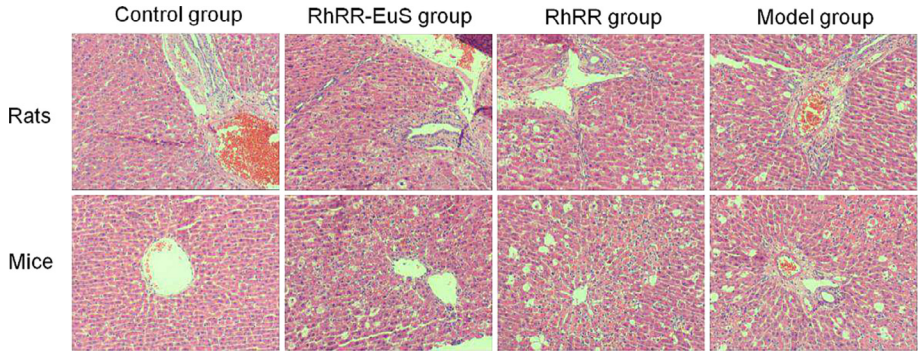

Fig. 6. Degree of acute liver injury in different groups of rats and mice.

and benzoic acid was mainly generated by aromatic acids and active polyphenols from the metabolic diet of microorganisms in the intestinal tract (Gong et al., 2017; Sheng et al., 2016). Phenylacetic acid was produced by the metabolism of amphetamines by intestinal anaerobes. Phenylacetylglycine was produced by the combination of phenylacetic acid and glycine in the liver. Trimethylamine was generated by choline under the action of intestinal flora, and then metabolized to trimethylamine oxide by hepatic flavin monooxygenase (Phetcharaburanin et al., 2016). Therefore, the level of hippuric acid in Model group was decreased, indicating that the balance of intestinal flora in mice was damaged. RhRR-EuS and RhRR could increase the level of hippuric acid, indicating that their hepatoprotective effects were generated by regulating the metabolism of intestinal flora.

5. Conclusion

In this study, we studied the protective effect of RhRR and RhRR-EuS drug pair on acute liver injury based on HPLC-MS/MS and ^{1}H NMR metabolomics. The pharmacokinetic effects of EuS on the main pharmacodynamic components of RhRR were comparatively analyzed. HPLC-MS/MS method was used to study the pharmacokinetic characteristics of five components in rats with normal and acute liver injury after oral administration of RhRR and RhRR-EuS decoction. The results showed that the active ingredients were more easily absorbed by the stomach and transfered into the blood after body injury, and the pathological state of acute liver injury in rats could selectively promote the absorption of some components. In addition, the ^{1}H NMR metabolomics combined with multivariate statistical analysis was used to explain the comprehensive characteristics of CCl_4-induced hepatic metabolic disorder in mice, which also confirmed that as the sovereign drug of DHCZP, the combination of RhRR-EuS could more effectively treat the hepatic injury in mice. Therefore, we elucidated the action mechanism of sovereign drug from DHCZP for the first time by combining the pharmacokinetic parameters of the main pharmacodynamic components with ^{1}H NMR metabolomics. This provided a reference for the clinical application of the classical prescription DHZCP, laid a solid theoretical basis for DHZCP in the diagnosis and treatment of liver diseases, and provided a more comprehensive scientific basis for the diagnosis and treatment of liver diseases.

CRediT authorship contribution statement

Gang Feng: Writing – original draft. **Jianli Bi:** Writing – original draft. **Wenfang Jin:** Writing – review & editing. **Qi Wang:** Writing – review & editing. **Zhaokui Dan:** Writing – review & editing. **Baolei Fan:** Writing – review & editing.

Declaration of Competing Interest

The authors declare that they have no known competing financial interests or personal relationships that could have appeared to influence the work reported in this paper.

Acknowledgments

This work was supported by the Key R&D Plan of Hubei Province for local special support in the field of general health (No. 2022BCE066).

References

An, Z., Hu, T., Lv, Y., Li, P., & Liu, L. (2019). Targeted amino acid and related amines analysis based on iTRAQ®-LC-MS/MS for discovering potential hepatotoxicity biomarkers. *Journal of Pharmaceutical and Biomedical Analysis, 178*, 112812–112840.

Cai, Y., Zheng, Q., Sun, R., Wu, J., Li, X., & Liu, R. (2020). Recent progress in the study of Artemisiae Scopariae Herba (Yin Chen), a promising medicinal herb for liver diseases. *Biomedicine & Pharmacotherapy, 130*, 110513–110527.

Chen, T. T., DU, S. L., Wang, S. J., Wu, L., & Yin, L. (2022). Dahuang Zhechong pills inhibit liver cancer growth in a mouse model by reversing Treg/Th1 balance. *Chinese Journal of Natural Medicines, 20*(2), 102–110.

Chinese Pharmacopoeia Commission (2020). *Pharmacopoeia of the People's Republic of China*. Beijing: China Medical Science and Technology Press.

Gao, X., Liu, Y., An, Z., & Ni, J. (2021). Active components and pharmacological effects of Cornus officinalis: Literature review. *Frontiers in Pharmacology, 12*, 513–525.

Gong, M. J., Wu, S. J., Yue, H., Wang, S. M., Liang, S. W., & Zhou, Z. J. (2017). Metabonomic analysis of Hugan Tables on CCl_4-induced acute hepatic injury in rats based on ^{1}H-NMR. *Chinese Pharmacological Bulletin, 3*(12), 1766–1770.

Gong, Z., Lin, J., Zheng, J., Wei, L., Liu, L., Peng, Y., ... Hu, G. (2019). Dahuang zhechong pill attenuates CCl_4-induced rat liver fibrosis via the PI3K-Akt signaling pathway. *Journal of Cellular Biochemistry, 121*(2), 1431–1440.

Huang, L., Liu, X. D., Li, P. H., Wu, T. X., & Zhu, H. M. (2021). Researchprogress of Dahuang Zhechong Pill in liver diseases. *Chinese Journal of Integrated Traditional and Western Medicine on Digestion, 29*(5), 364–369.

Hughes, J. H., Upton, R. N., Reuter, S. E., Phelps, M. A., & Foster, D. J. R. (2019). Optimising time samples for determining area under the curve of pharmacokinetic data using non-compartmental analysis. *Journal of Pharmacy and Pharmacology, 71*(11), 1635–1644.

Jing, W. F., Bi, J. L., Xu, S., Rao, M. F., Wang, Q., Yuan, Y., & Fan, B. L. (2022). Metabolic regulation mechanism of *Aconiti Radix Cocta* extract in rats based on ^{1}H-NMR metabonomics. *Chinese Herbal Medicines, 14*(4), 602–611.

Li, T., Xu, S., Bi, J., Huang, S., Fan, B., & Qian, C. (2020). Metabolomics study of polysaccharide extracts from *Polygonatum sibiricum* in mice based on ^{1}H-NMR technology. *Journal of the Science of Food and Agriculture, 100*(12), 4627–4635.

Li, T., Li, C., & Si, M. X. (2018). Study on accelerated oxidation characteristics of coix seed oil based on ^{1}H-NMR and multivariate statistical analysis. *Chinese Journal of Analytical Chemistry, 41*(12), 2779–2783.

Li, Y., & Zhao, X. (2020). NMR-based plasma metabonomics in hyperlipidemia mice. *Analytical Methods, 12*(15), 1995–2001.

Li, Z. Y., Hao, E. W., Cao, R., Lin, S., Zou, L. H., Huang, T. Y., ... Deng, J. G. (2022). Analysis on internal mechanism of zedoary turmeric in treatment of liver cancer based on pharmacodynamic substances and pharmacodynamic groups. *Chinese Herbal Medicines, 14*(04), 479–493.

Miao, Z., Lai, Y., Zhao, Y., Chen, L., Zhou, J., Li, C., & Wang, Y. (2021). Protective property of scutellarin against liver injury induced by carbon tetrachloride in mice. *Frontiers in Pharmacology, 12*, 710692–710705.

Ni, Z. H., Wu, L., Cao, K. X., Zhang, X. Q., Wang, D. Y., Zeng, Y. W., ... Chen, Z. P. (2019). Investigation of the pharmacodynamic substances in dahuang zhechong pill that inhibit energy metabolism. *Journal of Ethnopharmacology, 251*, 112332–112363.

Phetcharaburanin, J., Lees, H., Marchesi, J. R., Nicholson, J. K., Holmes, E., Seyfried, F., & Li, J. V. (2016). Systemic characterization of an obese phenotype in the zucker rat model defining metabolic axes of energy metabolism and host-microbial interactions. *Journal of Proteome Research, 15*(6), 1897–1906.

Qian, A., Zhou, L., Shi, D. X., Pang, Z. R., & Lu, B. N. (2023). Portulaca oleracea alleviates CCl_4-induced acute liver injury by regulating hepatic S100A8 and S100A9. *Chinese Herbal Medicines, 15*(1), 110–116.

Rezzani, R., Franco, C., & Rodella, L. F. (2019). Curcumin as a therapeutic strategy in liver diseases. *Nutrients, 11*(10), 2498–2504.

Sheng, Y. H., Qiao, J. Y., Jin, R. M., Yao, G. T., Zhou, L., & Tang, L. M. (2016). Metabonomic study on early biomarkers of hepatic injury induced by ethanolic extract from *Rhizoma Dioscoreae Bulbiferae* in rats based on ^{1}H-NMR. *Chinese Journal of Pharmacology and Toxicology, 30*(4), 306–316.

Tian, C., Shao, Y., Jin, Z., Liang, Y., Li, C., Qu, C., ... Liu, M. (2021). The protective effect of rutin against lipopolysaccharide induced acute lung injury in mice based on the pharmacokinetic and pharmacodynamic combination model. *Journal of Pharmaceutical and Biomedical Analysis, 209*, 114480–114488.

Tian, Y. Y., Ma, B. B., Yu, S. Y., Li, Y. L., Pei, H. L., Tian, S. Q., ... Wang, Z. B. (2023). Clinical antitumor application and pharmacological mechanisms of Dahuang Zhechong Pill. *Chinese Herbal Medicines, 15*(2), 169–180.

Wang, R., Yang, Z., Zhang, J., Mu, J., Zhou, X., & Zhao, X. (2019). Liver injury induced by carbon tetrachloride in mice is prevented by the antioxidant capacity of Anji white tea polyphenols. *Antioxidants, 8*(3), 64–76.

Wang, Y., Bi, C., Pang, W., Liu, Y., Yuan, Y., Zhao, H., ... Li, Y. (2019). Plasma metabolic profiling analysis of gout party on acute gout arthritis rats based on UHPLC-Q-TOF/MS combined with multivariate statistical analysis. *International Journal of Molecular Sciences, 20*(22), 5753–5773.

Wu, L., Du, S., Yang, F., Ni, Z., Chen, Z., Liu, X., ... Qin, K. (2020). Simultaneous determination of nineteen compounds of Dahuang zhechong pill in rat plasma by UHPLC-MS/MS and its application in a pharmacokinetic study. *Journal of Chromatography B, 1151*, 122200–122206.

Wu, L., Yang, F. R., Xing, M. L., Lu, S. F., Chen, H. L., Yang, Q. W., ... Huang, Y. (2022). Multi-material basis and multi-mechanisms of the Dahuang Zhechong pill for regulating Treg/Th1 balance in hepatocellular carcinoma. *Phytomedicine, 2022*, 154055–154066.

Wu, P. X., Liang, S. F., He, Y. P., Lv, R., Yang, B. D., Wang, M., ... Sun, W. L. (2022). Network pharmacology analysis to explore mechanism of Three Flower Tea against nonalcoholic fatty liver disease with experimental support using high-fat diet-induced rats. *Chinese Herbal Medicines, 14*(2), 273–282.

Xiao, S. Y., Zhao, Z. W., Ding, Z. H., Chen, S. Q., & Du, B. F. (2020). Study on accelerated oxidation characteristics of coix seed oil based on ^{1}H-NMR and multivariate statistical analysis. *Chinese Journal of Analytical Chemistry, 48*(4), 551–558.

Yamamoto, H., Nakayama, Y., & Tsugawa, H. (2021). OS-PCA: Orthogonal smoothed principal component analysis applied to metabolome data. *Metabolites, 11*(3), 149–160.

Yang, JY., Li, M., Zhang, CL., & Liu, D. (2021). Pharmacological properties of baicalin on liver diseases: A narrative review. *Pharmacological Reports, 73*(5), 1230–1239.

Yu, X. T., Zhang, J. R., Sun, N., Qing, Y., Li, J. P., Zhu, Z., ... Zhao, L. B. (2017). Effects of co-administration with chrysin and naringenin on the pharmacokinetic of saquinavir in rats. *Chinese Pharmaceutical Journal, 52*(15), 1347–1351.

Zhang, G. P., & Wang, D. X. (2019). Simultaneous determination of 6 kinds of constituent in Dahuang Zhechong Pills by HPLC-PDA. *China Pharmacy, 30*(1), 54–58.

Zheng, L., Zeng, J., Liu, X., Xu, M., Wang, L., & Jiang, X. H. (2020). Introduction to commonly used software for pharmacokinetic studies. *Chinese Journal of Hospital Pharmacy, 40*(23), 2484–2489.

Zou, Q., Wang, N., Gao, Z., Xu, H., Yang, G., Zhang, T., ... Chen, X. (2020). Antioxidant and hepatoprotective effects against acute CCl_4-induced liver damage in mice from red-fleshed apple flesh flavonoid extract. *Journal of Food Science, 85*(10), 3618–3627.